# Incorporating the subgrid-scale variability of clouds in the autoconversion parameterization using a PDF-scheme

T. Weber[1,2] and J. Quaas[1,3]

Received 2 February 2012; revised 10 October 2012; accepted 14 October 2012; published 13 November 2012.

[1] An investigation of the impact of the subgrid-scale variability of cloud liquid water on the autoconversion process as parameterized in a general circulation model is presented in this paper. For this purpose, a prognostic statistical probability density distribution (PDF) of the subgrid scale variability of cloud water is incorporated in a continuous autoconversion parameterization. Thus, the revised autoconversion rate is calculated by an integral of the autoconversion equation over the PDF of total water mixing ratio from the saturation vapor mixing ratio to the maximum of total water mixing ratio. An evaluation of the new autoconversion parameterization is carried out by means of one year simulations with the ECHAM5 climate model. The results indicate that the new autoconversion scheme causes an increase of the frequency of occurrence of high autoconversion rates and a decrease of low ones compared to the original scheme. This expected result is due to the emphasis on areas of high cloud liquid water in the new approach, and the non-linearity of the autoconversion with respect to liquid water mixing ratio. A similar trend as in the autoconversion is observed in the accretion process resulting from the coupling of both processes. As a consequence of the altered autoconversion, large-scale surface precipitation also shows a shift of occurrence from lower to higher rates. The vertically integrated cloud liquid water estimated by the model shows slight improvements compared to satellite data. Most importantly, the artificial tuning factor for autoconversion in the continuous parameterization could be reduced by almost an order of magnitude using the revised parameterization.

**Citation:** Weber, T., and J. Quaas (2012), Incorporating the subgrid-scale variability of clouds in the autoconversion parameterization using a PDF-scheme, *J. Adv. Model. Earth Syst.*, *4*, M11003, doi:10.1029/2012MS000156.

## 1. Introduction

[2] Low level clouds are important regulators in the climate system due to their cooling radiative effect [*Chen and Cotton*, 1987; *Bretherton et al.*, 2004]. The radiative properties of these so-called warm clouds (those containing no ice) are defined by the size distribution of their droplets and the horizontal and vertical distribution of cloud liquid water. A dominant physical process in warm clouds is the autoconversion (coagulation) of cloud droplets determining the precipitation formation, and consequently cloud liquid water and cloud cover. Moreover, the autoconversion is the initiating process, which is requisite for the following precipitation generating processes such as accretion (collecting cloud droplets by raindrops) or self-collection of raindrops.

[3] Usually, two approaches are applied to simulate the autoconversion process in general circulation models (GCMs). One uses a threshold mean droplet radius above which autoconversion of cloud droplets occurs to account for the strong non-linearity of the coalescence [*Sundqvist*, 1978; *Boucher et al.*, 1995; *Rotstayn*, 1997]. The other approach is a continuous parameterization coupling the cloud liquid water and the cloud droplet number concentration directly. This kind of parameterization can be derived from the stochastic collection equation describing the time evolution of a droplet spectrum [*Beheng*, 1994; *Lohmann and Roeckner*, 1996]. Another parameterization for autoconversion in a large-eddy simulation (LES) was developed by *Khairoutdinov and Kogan* [2000] using a regression analysis of simulated drop spectra. Although this formulation was derived only for the use in an LES, *Posselt and Lohmann* [2008] showed in their work that it is also applicable in a GCM.

[4] The autoconversion as a local process takes place on a subgrid-scale, but it is parameterized by means of

[1]Max Planck Institute for Meteorology, Hamburg, Germany.
[2]Now at Climate Service Center, Helmholtz-Zentrum Geesthacht, Hamburg, Germany.
[3]Now at Institute for Meteorology, Universität Leipzig, Leipzig, Germany.


1942-2466/12/2012MS000156

grid-box mean values. This introduces a bias since autoconversion is a non-linear process. *Wood et al.* [2002] found that the bias in the autoconversion rate caused by neglecting the subgrid-scale variability becomes the larger the coarser the resolution of the model grid is. Furthermore, these biases become strengthened the more pronounced the non-linearity is [*Pincus and Klein*, 2000]. *Wood et al.* [2002] showed that autoconversion rates differ by two-order of magnitudes among climate models and cloud-resolving models that participated in a single column model intercomparison study. It is not surprising that the autoconversion process contributes to the uncertainty of modeled climate scenarios.

[5] The tuning of autoconversion [*Rotstayn*, 2000] intends to obtain realistic accumulated precipitation in comparison to rain gauge networks or satellite retrievals. In coarse GCMs, this is achieved by too frequent precipitation of too low intensity. For example, *Nam and Quaas* [2012] found much higher frequencies of occurrence of precipitation in the ECHAM5 climate model compared to CloudSat satellite retrievals. A similar issue was reported by *Stephens et al.* [2010], who evaluated five different global climate and weather prediction models regarding their simulation of precipitation over the oceans. The investigation reveals that the models produce precipitation too frequent and too light compared to observations. The described problems of modeled precipitation frequencies and intensities can be a result of neglecting the subgrid-scale variability of cloud condensate. Replacing the mean cloud liquid water in the precipitation parameterization by a simulated distribution of cloud liquid water for each model grid-box may reduce the afore-mentioned biases. This can be achieved by applying a PDF of total water mixing ratio emphasizing isolated areas of cloud liquid water, i.e., inhomogeneous cloud fields within a grid-box of GCM. Thus, an increase of occurrence of higher autoconversion rates and a decrease of lower ones is expected.

[6] Several approaches were made to reduce the bias caused by neglecting the subgrid-scale variability of clouds. *Rotstayn* [2000] was able to increase the critical threshold parameter to a more realistic value by restricting the occurrence of autoconversion to the grid-box fraction determined cloudy by a triangular PDF of total water mixing ratio. A direct incorporation of inhomogeneity within clouds in the continuous autoconversion parameterization derived by *Beheng* [1994] was made by *Zhang et al.* [2002]. They used a PDF of a Gaussian distribution to introduce the in-cloud variability of cloud liquid water in autoconversion process. The new scheme was implemented and tested in a Canadian Single Column Model and led to improvements in terms of liquid water path in three analyzed case studies.

[7] Another approach to account for the subgrid-scale variability of clouds and microphysical properties in stratiform precipitation formation was done by *Jess* [2010]. Simulations with the ECHAM5 climate model show an earlier onset of precipitation and better agreement with observations using a prescribed PDF determined by measurements which distribute cloud droplets and ice crystals over the cloudy sub-boxes. A more complex description for a warm-rain microphysics parameterization taking into account the subgrid-scale variability was developed by *Cheng and Xu* [2009]. They derived an analytical expression for autoconversion by integrating an equation for the autoconversion rate over a joint-double Gaussian PDF of vertical velocity, liquid water potential temperature, total water mixing ratio and perturbation of rainwater mixing ratio for simulations in a single column model (SCM). This approach is more applicable to cloud resolving models than GCMs because of the required input for determining the joint- double Gaussian PDF.

[8] In this paper, a revised continuous autoconversion parameterization for warm clouds in a GCM is presented which accounts for the subgrid-scale variability of cloud liquid water. The new parameterization combines the autoconversion parameterization derived by *Beheng* [1994] with the statistical PDF approach described by *Tompkins* [2002] using an integral of the autoconversion rate over the saturated part of the PDF. While the old autoconversion parameterization in the ECHAM5 model, which uses the grid-box mean of cloud liquid water, is not consistent with the cloud cover scheme applying already the statistical PDF approach, the new autoconversion parameterization solves this problem. The new scheme allows to vary the shape of the PDF of total water mixing ratio, which is determined through the skewness and distribution width. Accordingly, this revised autoconversion scheme is different to other approaches using simple PDFs [*Rotstayn*, 2000] or prescribed PDFs derived from measurements [*Jess*, 2010]. In contrast to the other studies mentioned, the approach comes at little additional computational effort, since the total-water PDF is already determined by semi-prognostic equations in the model, and since the approach taken integrates the autoconversion over the PDF, rather than numerically splitting each grid column into sub-columns. The main purpose of this study is to analyze the impact of the subgrid-scale variability of cloud liquid water on the autoconversion and precipitation process by means of global model simulations compared to other studies considering only certain cases exemplarily [*Zhang et al.*, 2002; *Cheng and Xu*, 2009; *Jess*, 2010; *Turner et al.*, 2011]. A further motivation for this study is to find a method to reduce the low precipitation rates being too frequent in the ECHAM5 model [*Nam and Quaas*, 2012]. The new scheme is evaluated and compared with the original autoconversion parameterization using sensitivity simulations in the ECHAM5 climate model. The modified autoconversion rate and its impact on accretion, vertically integrated cloud liquid water as well as on large-scale precipitation and their statistics are analyzed. In Section 2, the new autoconversion parameterization is introduced and compared with the original scheme. Section 3 describes the different model experiments and methods. The results of the model simulations are analyzed in Section 4, and a section on summary and discussion closes this investigation in Section 5.

## 2. Introducing the Subgrid-Scale Variability of Cloud Liquid Water

[9] In the current version of the ECHAM5 climate model [*Roeckner et al.*, 2003], the autoconversion rate $Q_{aut}$ derived from the stochastic collection equation given by *Beheng* [1994] (in SI units) is applied:

$$Q_{aut} = \alpha r_l^{4.7} \tag{1}$$

with

$$\alpha = \gamma_1 \left(6 \cdot 10^{28} n^{-1.7} \left(10^{-6} N_l\right)^{-3.3} \left(10^{-3} \rho\right)^{4.7}\right) \frac{1}{\rho} \tag{2}$$

where $\gamma_1$ is a "tunable" parameter determining the efficiency of the autoconversion process, and hence, cloud lifetime; $n(=10)$ is the width parameter of the initial cloud droplet spectrum, $N_l$ the cloud droplet concentration, $\rho$ the air density and $r_l$ the in-cloud liquid water.

[10] To incorporate the subgrid-scale variability of cloud liquid water into the autoconversion process, the PDF approach developed by *Tompkins* [2002] is used. The approach is already employed to incorporate the subgrid-scale variability of water vapor and cloud condensate in the cloud cover scheme in the model. The scheme uses a beta-function based PDF of total water mixing ratio to calculate the horizontal cloud fraction by an integral of the saturated part of a PDF. Following this statical approach, and assuming saturation within the cloud, the mean cloud liquid water $\bar{r}_l$ in warm clouds ($T > 0^\circ$C) is written by *Tompkins* [2002] as

$$\bar{r}_l = \int_{r_s}^{b} (r_t - r_s) G(r_t) dr_t. \tag{3}$$

[11] Thus, the mean cloud liquid water $\overline{r_l}$ is equal to the integral over the difference of the total water mixing ratio $r_t$ and the saturation vapor mixing ratio $r_s$, for the PDF of the beta-function $G$ from the saturation vapor mixing ratio to the maximum of the total water mixing ratio distribution, $b$. $G$ is defined by *Tompkins* [2002] as

$$G(r_t) = \frac{1}{B(p,q)} \frac{(r_t - a)^{p-1} (b - r_t)^{q-1}}{(b-a)^{p+q-1}}, \tag{4}$$

with

$$B(p,q) = \frac{\Gamma(p)\Gamma(q)}{\Gamma(p+q)}, \tag{5}$$

for $a \le r_t \le b$, $p > 0$, $q > 0$ and $\Gamma$ as the gamma function, $B$ the beta-function, $a$ and $b$ the minimum and maximum of the total water mixing ratio distribution, respectively, and $P$ and $q$ the shape parameters of the beta distribution. The constraint that equation (3) can only be applied for warm clouds is necessary to exclude the cloud ice from the cloud condensate, which is obtained by the integral of the saturated part of the PDF. The cloud liquid water in equation (1) is replaced by $r_t - r_s$ and integrated from $r_s$ to $b$. Consequently, the subgrid-scale variability of cloud liquid water is introduced in the autoconversion process and the in-cloud autoconversion rate turns to the mean value of a grid-box

$$\overline{Q}_{aut} = \alpha \int_{r_s}^{b} (r_t - r_s)^{4.7} G(r_t) dr_t. \tag{6}$$

[12] To obtain the autoconversion rate inside the cloud, equation (6) has to be divided by the cloud fraction $C$ of the respective grid-box:

$$Q_{aut} = \frac{\overline{Q}_{aut}}{C}. \tag{7}$$

[13] The implementation of this revised autoconversion scheme into the existing cloud module of the model requires an additional algorithm for numerical integration of the integral in equation (6) and the time-integration of the autoconversion rate (equation (1)), which has been done analytically in the original formulation. These two technical modifications are described in Appendix A. Moreover, in order to obtain the similar results as with the original autoconversion scheme, it was necessary to fine-tune the model using the constraint that at most 90 % of the cloud liquid water can be converted to precipitation in one timestep.

## 3. Methods and Data

[14] The revised autoconversion scheme was implemented in the cloud microphysics of the ECHAM5 climate model [*Roeckner et al.*, 2003] to analyze the impact of the subgrid-scale variability of cloud liquid water in the autoconversion parameterization derived by *Beheng* [1994]. For this purpose, one-year simulations with an hourly output interval were carried out with the ECHAM5 model after a three-month spin-up period. Five different model experiments were performed using a horizontal resolution of T42 ($2.8^\circ \times 2.8^\circ$ or approx. 310 km at the equator) and a vertical resolution of 19 levels with the uppermost pressure level at 10 hPa (T42L19). Observed monthly mean sea surface temperature and sea ice data of 2004 were used as boundary conditions for the model experiments as in AMIP [*Gates et al.*, 1999].

[15] In two control experiments, the autoconversion parameterization derived by *Beheng* [1994] (orig-b) and the autoconversion parameterization given by *Khairoutdinov and Kogan* [2000] (orig-kk) were used with the standard version of the ECHAM5 climate model [*Lohmann and Roeckner*, 1996]. The new autoconversion parameterization was applied with two different values of the autoconversion tuning parameter $\gamma_1$ in equation (1). In an untuned experiment (*rev*), $\gamma_1$ was set equal to 15 as in the standard ECHAM5 configuration and, in a retuned one (*adj*), equal to 2 which results in an approximate balance of the net radiation (sum of net shortwave and longwave fluxes) at the top of the atmosphere

(TOA). Moreover, in a further experiment labeled *kk*, the autoconversion parameterization derived by *Beheng* [1994] was replaced by an alternative parameterization $Q_{aut} = 1350(\overline{r_l}/C)^{2.47} N_l^{-1.79}$ developed by *Khairoutdinov and Kogan* [2000] in order to test whether the observed impact of the incorporated subgrid-scale variability of cloud liquid water is restricted to the original autoconversion parameterization. The implementation of the alternative parameterization was carried out in the same way as described in Section 2 and Appendix A using the equation for the in-cloud autoconversion rate:

$$\overline{Q}_{aut} = 1350 N_l^{-1.79} \int_{r_s}^{b} (r_t - r_s)^{2.47} G(r_t) dr_t. \qquad (8)$$

[16] In the experiment (*kk*) the factor in the equation for the autoconversion rate has not been changed and applied as proposed by *Khairoutdinov and Kogan* [2000].

[17] The modeled quantities autoconversion and accretion rate, liquid water path (LWP) and large-scale precipitation rate, which are affected by the modified autoconversion parameterization are compared to ones in the control experiment.

## 4. Results

### 4.1. Changes in Autoconversion

[18] A comparison of the new (*rev*) and the original (*orig–b*) autoconversion parameterization reveals considerable differences in the mean autoconversion rates (Table 1), in the range of the autoconversion rates and in the distribution of their occurrence (Figures 1a and 1d). The mean autoconversion rate (averaged over all cloudy grid-boxes of the entire 3D model domain for one year at hourly intervals) in the new scheme is 0.47 times lower than the one in the original scheme with 0.053 $10^{-6}$ kg kg$^{-1}$s$^{-1}$. In detail, the new autoconversion scheme produces fewer small rates (below $10^{-15}$ kg kg$^{-1}$s$^{-1}$) and notably more higher rates (between $10^{-15}$ and $10^{-7}$ kg kg$^{-1}$s$^{-1}$) than the original one. Only autoconversion rates higher than $10^{-7}$ kg kg$^{-1}$s$^{-1}$ are slightly more often generated by the original scheme, which is nevertheless dominate the mean value. In general, this result seems reliable, because the introduction of subgrid-scale variability of cloud liquid water should reduce the occurrence and increase the amount of autoconversion compared to the use of the grid-box mean values. The fact that some very high autoconversion rates occur less frequently in the revised version is due to some feedbacks in cloud processes.

[19] The impact of modified parameterizations of the new scheme can be seen in the mean values (Table 1) and occurrence distributions of the autoconversion rates (Figures 1b and 1d). In the retuned version of the scheme (*adj*), the mean autoconversion rate is 0.26 times lower than in the original scheme due to the decreased tuning factor from 15 to 2 in the autoconversion equation (1). Accordingly, its occurrence distribution is shifted to lower autoconversion rates and the maximum is somewhat lower compared to untuned version. The alternative autoconversion parameterization (*kk*) produces a mean autoconversion rate, which is 0.85 times lower related to original scheme, and the narrowest and highest occurrence distribution of all experiments. A direct comparison of the new and old scheme using the alternative autoconversion parameterization given by *Khairoutdinov and Kogan* [2000] (Figure 1c) shows that the observed shift of occurrence from lower to higher autoconversion rates is not limited to a particular representation of the autoconversion process, but a result of the introduction of the subgrid-scale variability of cloud liquid water into this process.

### 4.2. Impact on Accretion

[20] The autoconversion process in the model also affects the accretion process which can be seen in Table 1 and Figures 2a–2d. In the microphysics scheme in the model, the accretion rate $Q_{racl}$ derived from the stochastic collection equation [*Beheng*, 1994] is parameterized in two terms:

$$Q_{racl} = \min(C, C_{pr}) d_1 \left(\frac{\overline{r_l}}{C}\right) (\rho r_{rain} + \gamma_2 \rho Q_{aut} \Delta t), \qquad (9)$$

with $d_1 = 6$ m$^3$kg$^{-1}$s$^{-1}$, $\overline{r_l}/C$ as in-cloud liquid water, $\rho$ as air density and $\gamma_2$ as tunable parameter. The two terms consider the two contributions to the rain water within a grid-box at a given time-step, namely the rain water falling into the volume from above, and the rain water formed within the grid-box due to autoconversion in the given time-step. The first term simulates the falling mass mixing ratio of rain $r_{rain}$ into the covered part $C_{pr}$ of the grid-box, and the second one the rain production during

**Table 1.** Global Annual Mean Values of Quantities in Different Experiments (See Text for Descriptions of the Experiments) and Their Ratios of the Experiment Using the Original Scheme

| | Experiments | | | | | | |
|---|---|---|---|---|---|---|---|
| | orig-b | rev | | adj | | kk | |
| Quantity | Mean | Mean | Ratio | Mean | Ratio | Mean | Ratio |
| Autoconv. Rate [$10^{-6}$kg kg$^{-1}$s$^{-1}$] | 0.023 | 0.009 | 0.39 | 0.006 | 0.26 | 0.015 | 0.65 |
| Autoconv. Rate [$10^{-6}$kg kg$^{-1}$s$^{-1}$] (cldy) | 0.053 | 0.025 | 0.47 | 0.014 | 0.26 | 0.045 | 0.85 |
| Accretion Rate [$10^{-6}$kg kg$^{-1}$s$^{-1}$] | 0.004 | 0.012 | 3.00 | 0.009 | 2.25 | 0.016 | 4.00 |
| Accretion Rate [$10^{-6}$kg kg$^{-1}$s$^{-1}$] (cldy) | 0.010 | 0.033 | 3.30 | 0.023 | 2.30 | 0.046 | 4.60 |
| LWP [gm$^{-2}$] | 61 | 50 | 0.82 | 82 | 1.34 | 57 | 0.93 |
| Large-Scale Precip. [mmh$^{-1}$] | 0.047 | 0.047 | 1.00 | 0.046 | 0.98 | 0.047 | 1.00 |
| Convective Precip. [mmh$^{-1}$] | 0.074 | 0.073 | 0.99 | 0.073 | 0.99 | 0.072 | 0.97 |

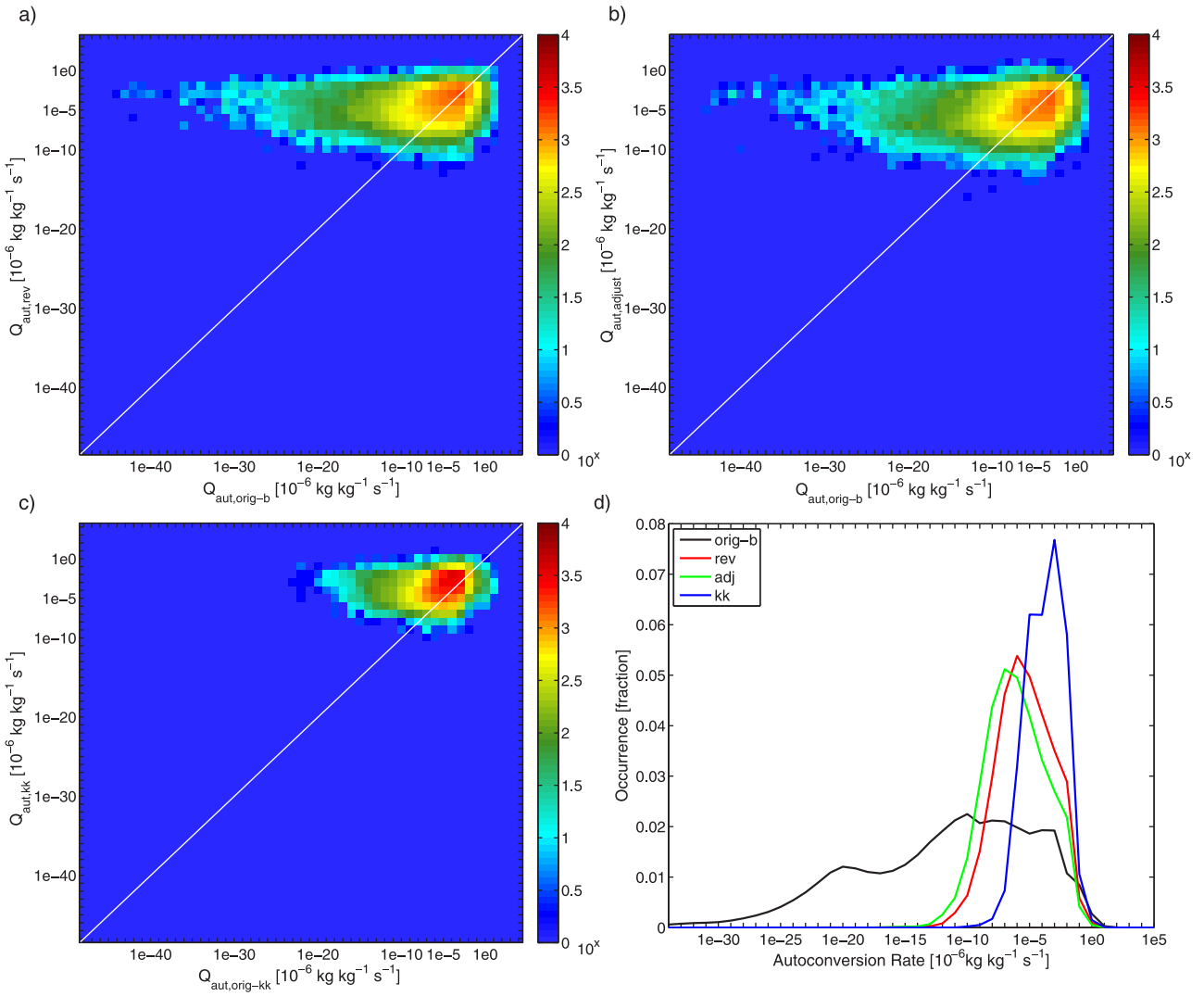


**Figure 1.** Six-hourly joint-histograms of in-cloud autoconversion rates from all model levels, (a) untuned version of new scheme (*rev*) against the original scheme (*orig-b*), (b) retuned version of the new scheme (*adjust*) against the original scheme (*orig-b*) and (c) an alternative parameterization (*kk*) against the original scheme (*orig-kk*). (d) Distribution of in-cloud autoconversion rates calculated by the original scheme (*orig-b*), the untuned (*rev*) and retuned (*adj*) version of the new scheme as well as by an alternative autoconversion parameterization (*kk*) from all model levels of one year.

the timestep $\Delta t$ by autoconversion. Consequently, the accretion rate contains the autoconversion rate directly, but it is also included indirectly by rain generated via autoconversion and decreased cloud liquid water.

[21] The mean accretion rate (averaged over all cloudy grid-boxes of the entire 3D model domain for one year at hourly intervals) is increased by a factor of 3.3 using the new autoconversion scheme (*rev*) compared to the original scheme (*orig–b*). This can be mainly explained with the increase of cloud liquid water in the lower atmosphere in the high latitudes where the highest amount of cloud liquid water occurs (Figures 3a and 3b). The maximum of the occurrence distribution of the accretion is slightly shifted to lower rates, but the maximum broadened over a larger range of accretion rates (also to higher values). Moreover, a reduction of the occurrence of low rates occurs when applying the new autoconversion scheme. These findings can be explained by the increased occurrence of high autoconversion rates represented in the second term of equation (9). The fact that the retuned experiment (*adj*) shows a quite similar distribution of accretion rates with higher mean cloud liquid water than in the untuned experiment (see Section 4.3) (Figures 2a and 2b) implies that the collection process of cloud droplets by falling raindrops plays only a secondary role.

[22] Changes in the mean rate and the distribution of the accretion rate can also be seen in the modified parameterizations of the new autoconversion scheme (Figures 2b and 2c). The maximum occurrence of accretion rates in the retuned version of the scheme (*adj*) is somewhat lower and the left side of its distribution tends towards lower rates compared to the untuned one (*rev*). As a result, the mean rate is 2.3 times higher than the one in the original scheme. The alternative autoconversion

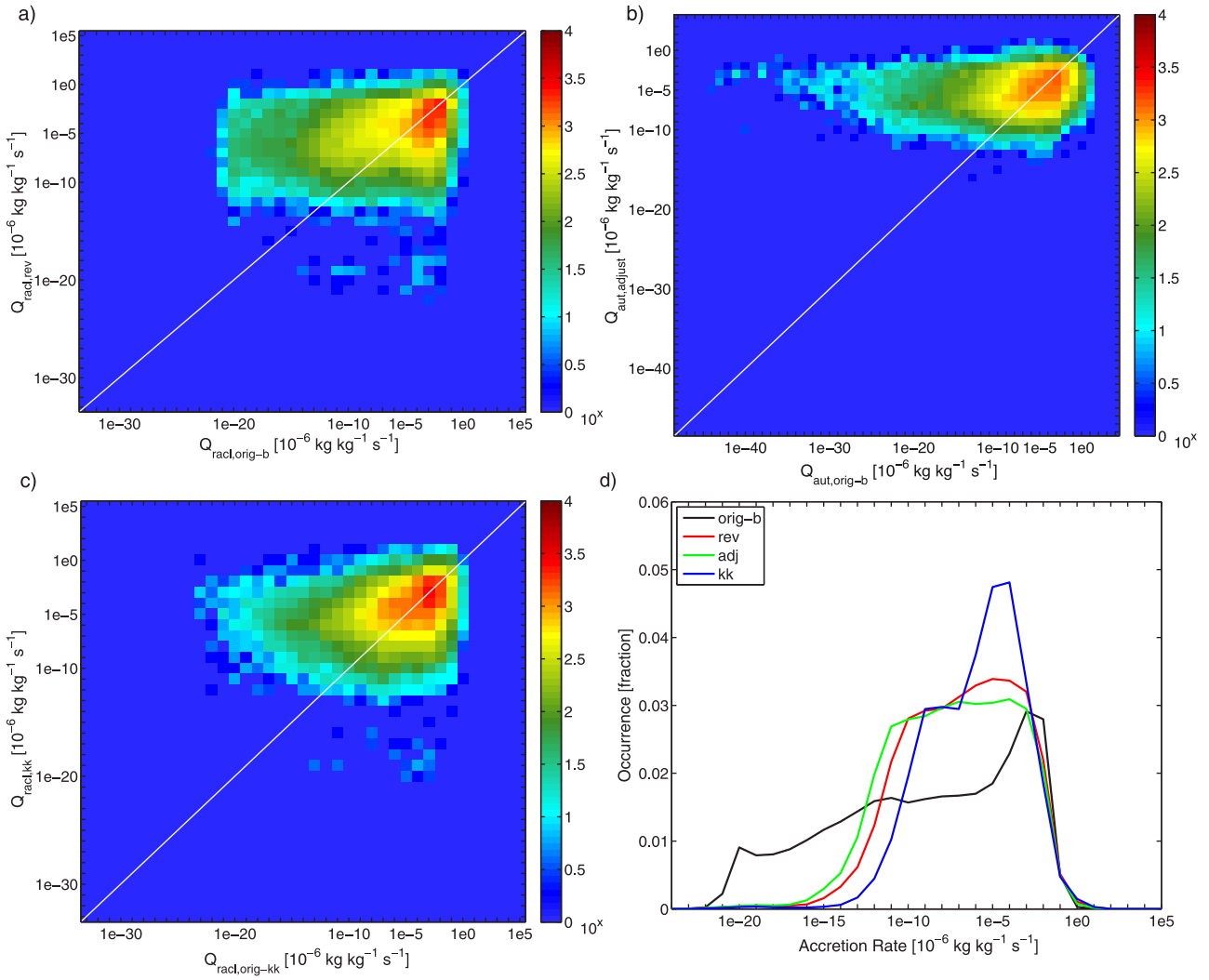


**Figure 2.** Six-hourly joint-histograms of in-cloud accretion rates from all model levels, (a) untuned version of new scheme (*rev*) against the original scheme (*orig-b*), (b) retuned version of the new scheme (*adjust*) against the original scheme (*orig-b*) and (c) an alternative parameterization (*kk*) against the original scheme (*orig-kk*). (d) Distribution of in-cloud accretion rates calculated by the original scheme (*orig-b*), the untuned (*rev*) and retuned (*adj*) version of the new scheme as well as by an alternative autoconversion parameterization (*kk*) from all model levels of one year.

parameterization (*kk*) exhibits a higher occurrence maximum than the untuned and retuned version, and the left side of the occurrence distribution is shifted towards higher rates. Thus this scheme simulates the highest mean accretion rate with a factor of 4.6 above the mean of the original scheme caused by the strong increase of cloud liquid water in the lower and middle atmosphere (Figure 3d). The indirect impact of the modified autoconversion scheme on the accretion rate can also be seen in the parameterization derived by *Khairoutdinov and Kogan* [2000] (Figure 2c) which is a result of the accretion formulation in the model.

### 4.3. Impact on Cloud Liquid Water

[23] A modification of the autoconversion process in the model has a direct impact on the bulk of cloud liquid water, but also the accretion process modified again by the autoconversion of cloud droplets affects the cloud liquid water as explained before in Section 4.2. Increasing the cloud liquid water flow in both processes decreases the liquid cloud water, but the autoconversion is generally the more important one since it initiates the precipitation process in warm clouds. Furthermore, it should be noticed that the precipitation generation in convective clouds, and the precipitation originating from mixed-phase and ice clouds, all of which are not directly affected by this parameterization change, also have a substantial impact on the cloud liquid water. In the experiment using the untuned version (*rev*) of the new autoconversion scheme, the mean LWP is 0.82 times lower than the one applying the original scheme (*orig–b*) with 61 gm$^{-2}$. This seems curious since the mean autoconversion rate is also decreased in this experiment. However, at the same time, the mean accretion rate is increased by a factor of 3.37 overcompensating the reduction in the autoconversion. A different result is obtained when the autoconversion is further decreased as in the retuned experiment (*adj*). In this one,

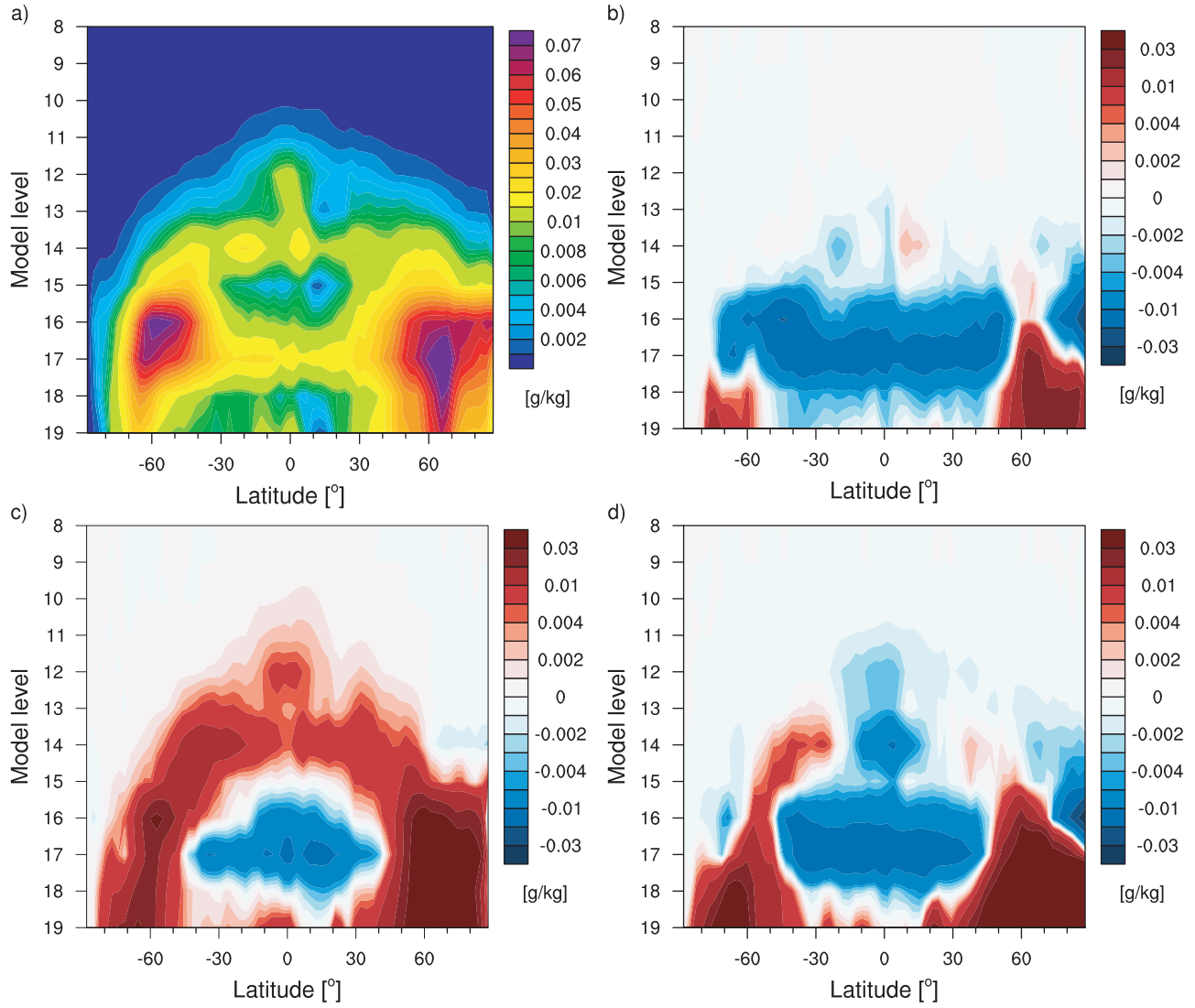


**Figure 3.** (a) Vertical distribution of zonal annual mean cloud liquid water calculated by the original scheme (*orig-b*), (b) untuned version of the new scheme (*rev*) minus the original scheme (*orig-b*), (c) retuned version of the new scheme (*adjust*) minus the original scheme (*orig-b*) and (d) an alternative parameterization (*kk*) minus the original scheme (*orig-b*).

the mean LWP is increased by a factor of 1.34, whereas the mean accretion rate is lower than in the untuned one and increased only by a factor of 2.29 compared to the control experiment. This implies that at a certain amount of autoconversion the accretion process does not (over)compensate the reduction of the autoconversion anymore.

[24] The zonal mean distribution of the LWP simulated by the untuned version of the new autoconversion scheme is always lower than the one by the original scheme, except for the region around 60° N where the untuned scheme retains more cloud liquid water in the atmosphere (Figure 4). In order to asses roughly the changes in LWP simulated by the model compared to observational data, the column liquid cloud water from MODIS Atmosphere L3 Gridded Products (Liquid Water Cloud Water Path: Level-2 Quality Assurance Weighted Mean) is used with a horizontal resolution of 1°. This L3 variable was calculated applying the Quality Assurance weighting information from the L2 product [*King et al.*, 2003]. A general increase of cloud liquid water in all regions can be observed in the retuned experiment, which gives a better agreement with the MODIS-derived column liquid cloud water compared to the original scheme. The very high cloud liquid water in the polar regions shown in the observational data may be unrealistic and due to the retrieval methods of MODIS [*Seethala and Horváth*, 2010]. However, the retuned new autoconversion scheme overestimates the cloud liquid water somewhat around 60° N. The fact that both untuned and the retuned version of the new scheme show higher values of cloud liquid water around 60° N than the control experiment may be related to deficiencies in the parameterization of the simulated PDF of total water mixing ratio over land [*Weber et al.*, 2011]. The LWP simulated with the alternative autoconversion parameterization (*kk*) (Figure 4)

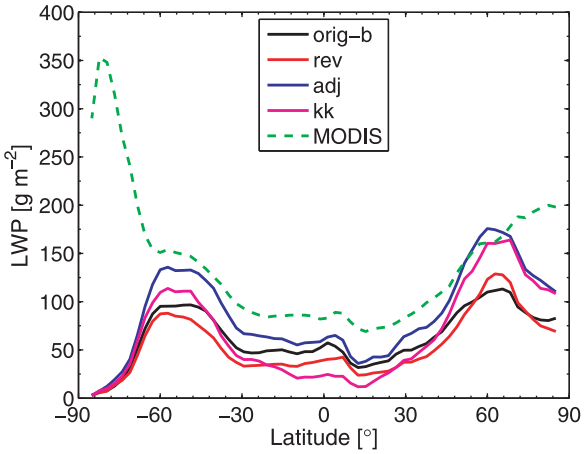


**Figure 4.** Comparison of the zonal annual mean of LWP simulated by the original autoconversion (*orig-b*), and the untuned (*rev*) and retuned (*adj*), and untuned (*kk*) version of the new autoconversion scheme as well as the column liquid cloud water derived from MODIS satellite data.

indicates that there is still a need for a tuning factor even when this LWP is closer to the observations in the high latitudes.

[25] The new scheme leads to an increase of cloud liquid water in the lower atmosphere over the high latitudes and to a reduction in the mid-latitudes and Tropics caused by feedbacks between the autoconversion process and cloud liquid water (Figures 3a–3d). Interestingly, the reduction of the tuning factor in the retuned experiment (*adjust*) results in an increase of cloud liquid water in the middle atmosphere over the mid-latitudes and Tropics (Figure 3c), which may caused by the non-linearity of the cloud liquid water term in the autoconversion process.

### 4.4. Impact on Large-Scale Precipitation

[26] The autoconversion of cloud droplets to raindrops in warm ($T>0°C$) and mixed phased clouds ($-35°C \leq T < 0°C$) is the crucial process for generating large-scale precipitation. On the one hand, it produces raindrops being the prerequisite for the accretion process (collection of cloud droplets by falling rain) and, on the other hand, it decreases directly the amount of cloud liquid water. The autoconversion also indirectly affects the accretional growth of falling snow by collecting cloud droplets. This microphysical process contributes also to the large-scale precipitation.

[27] The untuned version (*rev*) of the new autoconversion parameterization simulates almost the same mean large-scale precipitation rate $P$ as the original one (*orig–b*) with 0.047 mmh$^{-1}$ (with a negligible difference of $-0.0005$ mmh$^{-1}$), whereas the retuned version (*adj*) causes a small reduction by $-2.1$ %. Since surface temperatures, and thus to a first order also the evaporation rates, over oceans are fixed, the small differences are expected. The slight change in the *adj* version is due to a cooling of the land surfaces, and subsequent reduction in evaporation over land, due to the strong increase in cloud LWP. This increase by 34.4 % can not be explained solely by the small reduction of large-scale precipitation; rather it is due to the compensation of a reduction of convective precipitation over land in the Tropics following the land surface cooling.

[28] An analysis of changes in occurrence of large-scale precipitation in the model domain is made taking into account those rates being equal or larger to a value of 0.01 mmh$^{-1}$ at which precipitation is considered as measurable [*Glickman*, 2000]. Precipitation rates lower than 0.01 mmh$^{-1}$ contribute only 1.2 % to the accumulated precipitation, but have a frequency of occurrence of 65 %. This high value is a result of the fact that ECHAM5 artificially produces very small precipitation rates down to $10^{-15}$ mmh$^{-1}$ virtually always in hourly model output (which means that there is almost no grid-box where the precipitation rate is exactly zero). The artificial precipitation is a result of a missing threshold trigger value that initiates the formation of precipitation. A similar problem is observed in simulations of the HIRHAM regional climate model, whose convection scheme tends to artificially produce light precipitation [*May*, 2008].

[29] The precipitation rates are roughly classified in three categories, the characteristics of which are shown for the control experiment on a global scale (Figures 5a and 5b). The first category, low precipitation containing grid-boxes with rates between $0.01 \leq P \leq 0.1$ mmh$^{-1}$, has a frequency of occurrence of 24.5 % globally, and contributes 16.5 % to the accumulated precipitation in the control version of the model. Moderate precipitation rates classified by $0.01 \leq P \leq 1.0$ mmh$^{-1}$ contribute the most of all categories to accumulated precipitation with 56 %, but have a frequency of occurrence of only 9.7 %. The lowest occurrence with 0.7 %, but a contribution of 26.2 % to total precipitation, has the category labeled here as high precipitation rates containing grid-boxes with rates higher than 1.0 mmh$^{-1}$.

[30] Applying the new autoconversion scheme, the frequency of occurrence of low precipitation rates is decreased moderately by $-3.5$ % in the untuned experiment and considerably, by $-11.6$ %, in the retuned one (Figures 5c and 5d). Furthermore, in the retuned experiment, the occurrence of high precipitation rates is increased by 1.3 % in comparison to the control experiment (note that these numbers are for only the large-scale precipitation, not including the contribution by convective precipitation). The reduction of low precipitation rates and the increase of the high ones in the retuned experiment result from the shift of the autoconversion occurrence from lower to higher values (see Section 4.1).

## 5. Summary and Discussion

[31] A revised continuous autoconversion parameterization for warm clouds in a GCM accounting for the subgrid-scale variability of cloud liquid water is presented. The new parameterization combines the autoconversion by *Beheng* [1994] with the statistical approach developed by *Tompkins* [2002] using an integral of the autoconversion

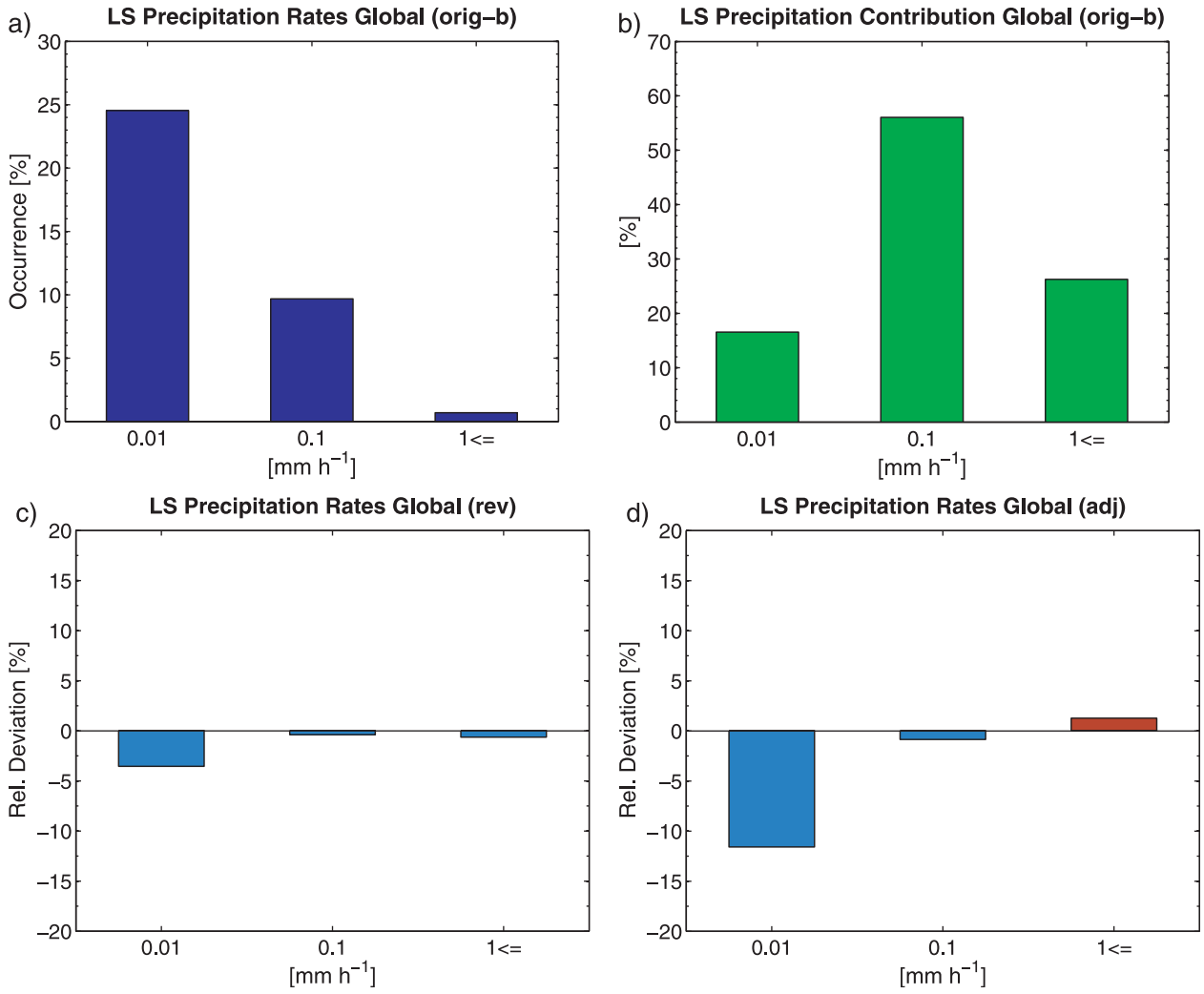


**Figure 5.** Global large-scale precipitation rates at the surface: (a) occurrence of precipitation rates by categories in the control experiment [%], (b) contribution of categories to the total amount [%] and deviation of occurrence [%] in the (c) untuned and (d) retuned experiment from the control experiment.

rate over the saturated part of the PDF of total water mixing ratio. The new scheme was implemented and applied in the ECHAM5 climate model in order to evaluate the impact of subgrid-scale variability of cloud liquid water on the autoconversion process. For this purpose model experiments with a horizontal resolution of $2.8^\circ \times 2.8^\circ$ (T42) and 19 vertical levels were carried out using the prescribed sea surface temperature and sea-ice distribution of 2004. Results obtained by the new autoconversion scheme were compared to the ones by the original parameterization considering the autoconversion rate and the affected quantities accretion rate, cloud liquid water and large-scale precipitation. Moreover, column liquid cloud water derived from MODIS was used to asses the simulated LWP.

[32] The results show that accounting for subgrid-scale variability of cloud liquid water in the autoconversion process leads to an increase of occurrence in higher autoconversion rates and to a reduction of lower ones compared to the parameterization using the mean cloud liquid water. This achievement is considered as improvement since it leads to a shift of the frequency of occurrence of large-scale precipitation from lower to higher rates, which was one of the aims of this study. The result can be explained with the applied PDF of total water mixing ratio simulating the distribution of cloud liquid water with horizontally inhomogeneous cloud fields in a model grid-box more realistically, i.e., emphasizing specific areas of high cloud liquid water (thick clouds).

[33] It is shown that the increase of occurrence in higher autoconversion rates and the reduction of lower ones are not limited to certain autoconversion parameterization [e.g., *Beheng*, 1994]. Similar results were achieved with an alternative autoconversion parameterization derived by *Khairoutdinov and Kogan* [2000] which has less sensitivity to cloud liquid water. This suggests that the incorporation of subgrid-scale variability of cloud liquid water in the autoconversion process will probably also lead to similar results with different autoconversion parameterizations in other models. We expect that threshold based schemes will behave similar

to the high-nonlinear Beheng's formulation [*Beheng*, 1994] because effectively they are also very non-linear in cloud water mixing ratio. A further important achievement is the reduction of the tuning factor in the autoconversion parameterization from 15 to 2. Thus the revised model allows for a tuning factor much closer to the "perfect" factor of 1.

[34] The modified autoconversion parameterization also causes a change in the distribution of accretion rates resulting from the coupling of both processes. The new distribution of the accretion rates resembles the one of the autoconversion rates with an increase of occurrence of higher rates and a decrease of lower ones compared to the original parametrization. Both autoconversion and accretion process affect the amount of cloud liquid water in the atmosphere. A general increase of cloud liquid water is observed in the lower atmosphere over the high latitudes and a reduction in cloud liquid water over the mid-latitudes and the Tropics. In particular, the revised model version simulates a much higher amount of cloud liquid water and, additionally, an increase of cloud liquid water in the middle atmosphere over the mid-latitudes and Tropics.

[35] The incorporation of subgrid-scale variability of cloud liquid water into the autoconversion parameterization for warm clouds causes a shift of the frequency of occurrence of large-scale precipitation from lower to higher rates. This achievement may lead to a reduction of the discrepancies between the occurrence of precipitation rates derived from CloudSat satellite retrievals and the modeled rates being overestimated for lower rates and underestimated for higher rates found by *Nam and Quaas* [2012]. A further improvement of the new autoconversion parameterization is the fact that the calculation of the cloud liquid water using the statistical PDF scheme by *Tompkins* [2002] is now consistent with cloud cover scheme, which already applies this statistical PDF approach.

[36] It is interesting to note the non-linearity of the response of precipitation to the modification of the autoconversion rate. The feedbacks of the cloud water path to the changes in autoconversion may yield either sign of the resulting precipitation to a reduction in initial autoconversion efficiency. This result may be important in the scientific debate about effects of anthropogenic aerosols on autoconversion rates, which commonly are interpreted as leading to reduced precipitation rates [*Albrecht*, 1989].

[37] However, it has to be mentioned that there are still differences between the modeled moments, variance and skewness, determining the PDF of total water mixing ratio and observations [*Weber et al.*, 2011]. This study found that the variance (distribution width) is globally underestimated over the continents in the low latitudes, and the skewness is overestimated in the Tropics by the subgrid-scale variability scheme producing positive skewness while observations show negative skewness in this region. Therefore, it is likely that the results achieved in this work will change in future when the deficiencies in the parameterization of these moments are corrected. Preliminary tests show that an increase of distribution width of the PDF and allowing negative skewness in the model will cause a further shift to higher autoconversion rates, and potentially to higher large-scale precipitation rates. Thus, the tuning factor in the autoconversion equation may be eliminated completely with an improved scheme of the subgrid- scale distribution of cloud water.

## Appendix A: Notes on Implementation of the New Autoconversion Scheme

[38] The autoconversion process is implemented in the cloud module, where cloud microphysics such as condensation and evaporation is determined. These processes have a strong impact on the bulk of cloud liquid water affecting the autoconversion rate. Since these processes are calculated before the autoconversion rate is computed, the in-cloud water is not anymore consistent with distribution width and skewness of total water mixing ratio and cloud fraction. Consequently, there is a need to recompute these quantities to obtain consistency for the use in the autoconversion scheme.

[39] Moreover, in the original autoconversion scheme, the calculation of the autoconversion rate and the time-integration are performed implicitly. Both procedures had to be separated using the third-order Runge-Kutta method for the time-integration before the implementation could be carried out. The third-order of the Runge-Kutta method was chosen because it gives the closest results to the formerly applied implicit time-integration compared to the first and second-order method. Because of the replacement of the implicit time-integration, it was necessary to implement a constraint that the entire cloud liquid water can not be converted to precipitation in one timestep. This constraint was set to 90 % being a result of model fine-tuning in order to get the same results as with the original model parameterization.

[40] A crucial point was to find an applicable integration method, which was easy to implement and had low computational costs. The Simpson's rule is a method for a numerical integration approximating a definite integral. Some tests of this method with different shapes of the PDF resulted in a good approximation with an error lower than 1 % using 100 supporting points. Because of the third-order Runge-Kutta time-integration, the integration of the saturated part of the PDF of total water mixing ratio has to be calculated three times. After each calculation, it is necessary to re-estimate the defining quantities (total water mixing ratio, its maximum and its skewness) of the PDF using the equations introduced by *Tompkins* [2002]. A change of cloud condensate $\Delta r_c^{mic}$ ($mic$ = microphysics) due to the autoconversion process results a change of the maximum of total water mixing ratio

$$\Delta b^{mic} = \frac{\Delta \bar{r}_c^{mic}}{\bar{r}_c}(b - r_s) \tag{A1}$$

with

$$\Delta \bar{r}_c^{mic} = \bar{r}_{c,n+1}^{mic} - \bar{r}_{c,n}^{mic}, \tag{A2}$$

where $b$ is the maximum of total water mixing ratio, $r_s$ the saturation mixing ratio (always equal higher to the

minimum of total water mixing ratio $a$ in cloudy situations considered here) and $r_c$ the cloud condensate. The index one below $r_c^{mic}$ represents the new mean cloud condensate after the first time-integration. Afterwards, $\Delta b^{mic}$ and the new total water mixing ratio $\bar{r}_{t,n+1}$ are used to calculate the new shape-parameter $q_{n+1}$

$$q_{n+1} = \frac{(b + \Delta b^{mic} - a)p}{\bar{r}_{t,n+1} - a} - p. \tag{A3}$$

$p$ is the shape-parameter being set constant equal 2 and $b$ the quantity containing the value before the time-integration. Then, the new $b_{n+1}$ can be estimated

$$b_{n+1} = (\bar{r}_{t,n+1} - a)\frac{p + q_{n+1}}{p} + a. \tag{A4}$$

[41] After the last time-integration, the autoconversion rate is divided by cloud fraction of the respective grid-box to relate the rate to the cloud.

[42] **Acknowledgments.** This work was supported by the German Research Foundation (Deutsche Forschungsgemeinschaft, DFG) by an "Emmy Noether" grant and was done in the framework of the International Max Planck Research School on Earth System Modelling (IMPRS-ESM). Computing time was provided by the German High Performance Computing Centre for Climate- and Earth System Research (Deutsches Klimarechenzentrum, DKRZ). MODIS data used in this study were acquired as part of NASAs Earth Science Enterprise. The MODIS Science Teams developed the algorithms for the AOD retrievals. The data were processed by the MODIS Adaptive Processing System and the Goddard Distributed Active Archive (DAAC). The authors would like to thank three anonymous reviewers, as well as Erich Roeckner, Ulrike Lohmann, Sebastian Rast, Verena Grützun and the members of the Cloud-Climate Feedbacks Group in the Max Planck Institute for Meteorology for useful discussions.

## References

Albrecht, B. A. (1989), Aerosols, cloud microphysics, and fractional cloudiness, *Science*, *245*, 1227–1230, doi:10.1126/science.245.4923.1227.

Beheng, K. D. (1994), A parameterization of warm cloud microphysical conversion processes, *Atmos. Res.*, *33*, 193–206, doi:10.1016/0169-8095(94)90020-5.

Boucher, O., H. Le Treut, and M. B. Baker (1995), Precipitation and radiation modeling in a general circulation model: Introduction of cloud microphysical processes, *J. Geophys. Res.*, *100*(D8), 16,395–16,414, doi:10.1029/95JD01382.

Bretherton, C. S., T. Uttal, C. W. Fairall, S. E. Yuter, R. A. Weller, D. Baumgardner, K. Comstock, R. Wood, and G. B. Raga (2004), The EPIC 2001 stratocumulus study, *Bull. Am. Meteorol. Soc.*, *85*(7), 967–977, doi:10.1175/BAMS-85-7-967.

Chen, C., and W. R. Cotton (1987), The physics of the marine stratocumulus-capped mixed layer, *J. Atmos. Sci.*, *44*, 2951–2977, doi:10.1175/1520-0469(1987)044<2951:TPOTMS>2.0.CO;2.

Cheng, A., and K.-M. Xu (2009), A PDF-based microphysics parameterization for simulation of drizzling boundary layer clouds, *J. Atmos. Sci.*, *66*, 2317–2334, doi:10.1175/2009JAS2944.1.

Gates, W. L., et al. (1999), An overview of the results of the Atmospheric Model Intercomparison Project (AMIP I), *Bull. Am. Meteorol. Soc.*, *80*(1), 29–55, doi:10.1175/1520-0477(1999)080<0029:AOOTRO>2.0.CO;2.

Glickman, T. S. (2000), *AMS Glossary of Meteorology*, 2nd ed., Am. Meteorol. Soc., University Park, Pa.

Jess, S. (2010), Impact of subgrid variability on large-scale precipitation formation in the climate model ECHAM5, PhD thesis, Dep. of Environ. Syst. Sci., ETH Zurich, Zurich, Switzerland.

Khairoutdinov, M., and Y. Kogan (2000), A new cloud physics parameterization in a large-eddy simulation model of marine stratocumulus, *Mon. Weather Rev.*, *128*, 229–243, doi:10.1175/1520-0493(2000)128<0229:ANCPPI>2.0.CO;2.

King, M. D., W. P. Menzel, Y. J. Kaufman, D. Tanre, B.-C. Gao, S. Platnick, S. A. Ackerman, L. A. Remer, R. Pincus, and P. A. Hubanks (2003), Cloud and aerosol properties, precipitable water, and profiles of temperature and water vapor from MODIS, *IEEE Trans. Geosci. Remote Sens.*, *41*(2), 442–458, doi:10.1109/TGRS.2002.808226.

Lohmann, U., and E. Roeckner (1996), Design and performance of a new cloud microphysics scheme developed for the ECHAM general circulation model, *Clim. Dyn.*, *12*, 557–572, doi:10.1007/BF00207939.

May, W. (2008), Potential future changes in the characteristics of daily precipitation in europe simulated by the HIRHAM regional climate model, *Clim. Dyn.*, *30*, 581–603, doi:10.1007/s00382-007-0309-y.

Nam, C., and J. Quaas (2012), Evaluation of clouds and precipitation in the ECHAM5 general circulation model using CALIPSO and CloudSat satellite data, *J. Clim.*, *25*, 4975–4992, doi:10.1175/JCLI-D-11-00347.1.

Pincus, R., and S. A. Klein (2000), Unresolved spatial variability and microphysical process rates in large-scale models, *J. Geophys. Res.*, *105*, 27,059–27,065, doi:10.1029/2000JD900504.

Posselt, R., and U. Lohmann (2008), Introduction of prognostic rain in ECHAM5: Design and single column model simulations, *Atmos. Chem. Phys.*, *8*, 2949–2963, doi:10.5194/acp-8-2949-2008.

Roeckner, E., et al. (2003), The atmospheric general circulation model ECHAM5 part I: Model description, *Rep. 349*, Max Planck Inst. for Meteorol., Hamburg, Germany.

Rotstayn, L. D. (1997), A physically based scheme for the treatment of stratiform clouds and precipitation in large-scale models. I: Description and evaluation of the microphysical processes, *Q. J. R. Meteorol. Soc.*, *123*, 1227–1282.

Rotstayn, L. D. (2000), On the "tuning" of autoconversion parameterization in climate models, *J. Geophys. Res.*, *105*, 15,495–15,507, doi:10.1029/2000JD900129.

Seethala, C., and Á. Horáth (2010), Global assessment of AMSR-E and MODIS cloud liquid water path retrievals in warm oceanic clouds, *J. Geophys. Res.*, *115*, D13202, doi:10.1029/2009JD012662.

Stephens, G. L., T. L'Ecuyer, R. Forbes, A. Gettlemen, J.-C. Golaz, A. Bodas-Salcedo, K. Suzuki, P. Gabriel, and J. Haynes (2010), Dreary state of precipitation in global models, *J. Geophys. Res.*, *115*, D24211, doi:10.1029/2010JD014532.

Sundqvist, H. (1978), A parameterization scheme for non-convective condensation including prediction of cloud water content, *Q. J. R. Meteorol. Soc.*, *104*, 677–690, doi:10.1002/qj.49710444110.

Tompkins, A. M. (2002), A prognostic parameterization for the subgrid-scale variability of water vapor and clouds in large-scale models and its use to diagnose cloud cover, *J. Atmos. Sci.*, *59*(12), 1917–1942, doi:10.1175/1520-0469(2002)059<1917:APPFTS>2.0.CO;2.

Turner, S., J.-L. Brenguier, and C. Lac (2011), A subgrid parameterization scheme for precipitation, *Geosci. Model Dev. Discuss.*, *4*(3), 1643–1684, doi:10.5194/gmdd-4-1643-2011.

Weber, T., J. Quaas, and P. Räisänen (2011), Evaluation of the statistical cloud scheme in the ECHAM5 model using satellite data, *Q. J. R. Meteorol. Soc.*, *137*, 2079–2091, doi:10.1002/qj.887.

Wood, R., P. R. Field, and W. R. Cotton (2002), Autoconversion rate bias in stratiform boundary layer cloud parameterization, *Atmos. Res.*, *65*, 109–128, doi:10.1016/S0169-8095(02)00071-6.

Zhang, J., U. Lohmann, and B. Lin (2002), A new statistically based autoconversion rate parameterization for use in large-scale models, *J. Geophys. Res.*, *107*(D24), 4750, doi:10.1029/2001JD001484.

Corresponding author: T. Weber, Climate Service Center, Helmholtz-Zentrum Geesthacht, Fischertwiete 1, D-20095 Hamburg, Germany. (torsten.weber@hzg.de)